JOURNAL OF MATERIALS SCIENCE 17 (1982) 1997–2003

Characterization of silicon-enriched layers on nickel obtained by chemical vapour deposition

J. SUBRAHMANYAM
Materials Science Laboratory, BHEL Corporate Research and Development Division, Vikasnagar, Hyderabad 500 593, India

Silicon-enriched layers were developed on pure nickel by hydrogen reduction of silicon tetrachloride in the temperature range 950 to 1080° C. Depending on the deposition parameters, two types of layers formed on the surface: Type I consisted of solid solution of silicon in nickel and Type II showed several phases. The latter type exhibits a stone-like surface morphology. Short-time oxidation tests conducted using a thermobalance show that the coated specimens have improved oxidation resistance compared to pure nickel.

1. Introduction

Silicides are highly suitable materials for preventing oxidation at high temperatures. The silicide layers as coatings on refractory metals like molybdenum are well known. Recently, considerable attention has been directed towards obtaining silicon enriched layers on nickel-based superalloys as a protection against hot corrosion and oxidation. Chemical vapour deposition (CVD) of silicon-enriched layers can be accomplished by hydrogen reduction of silicon tetrachloride on a heated substrate. Most of the earlier work was concerned with the deposition of silicon on nickel-based superalloys [1–4]. The deposition process on these alloys is very complicated since alloying elements in nickel can either catalyse or retard the reaction on the surface and some of the alloying elements can diffuse out into the coating, affecting the deposition process.

In the present investigation silicon-enriched layers were developed on pure nickel substrates, by hydrogen reduction of silicon tetrachloride in the temperature range of 950 to 1080° C. The hydrogen partial pressures were kept relatively high ($p_{H_2} > 0.8$), so that reduction reactions are preferred compared to metal replacement reactions. Deposits were characterized using X-ray diffraction analysis, scanning electron microscopy, electron-probe microanalysis and short-time oxidation tests.

2. Experimental details

High-purity argon and hydrogen gases (obtained from Indian Oxygen Ltd) were used in the experiments without further purification. Silicon tetrachloride (supplied by Mettur Chemicals) was further purified by distillation. Electrolytic nickel was used as substrate samples. A schematic diagram of the experimental set-up is shown in Fig. 1. The vapours of silicon tetrachloride were transported to the reaction site by passing argon over the liquid, kept immersed in a constant temperature bath. A vertically mounted resistance furnace was used to heat the substrates to the required temperature. The substrates were heated to the desired temperature in argon atmosphere. Deposition was started by passing the gas mixture of hydrogen and silicon tetrachloride over the substrates. The deposition was terminated by closing the gas mixture and the samples were cooled in argon atomosphere to room temperature.

Scanning electron micrographs were taken using a Cambridge SEM and the X-ray diffraction analysis was carried out using Phillips X-ray diffractometer. The electron-probe microanalysis was conducted using a CAMECA electron-probe microanalyser. Oxidation experiments were carried out in an atmosphere of commercially-pure oxygen. These experiments were performed at 1000° C at an oxygen flow rate of 6.4 ml min^{-1}. The weight change with time was continuously recorded

0022–2461/82/071997–07$03.34/0

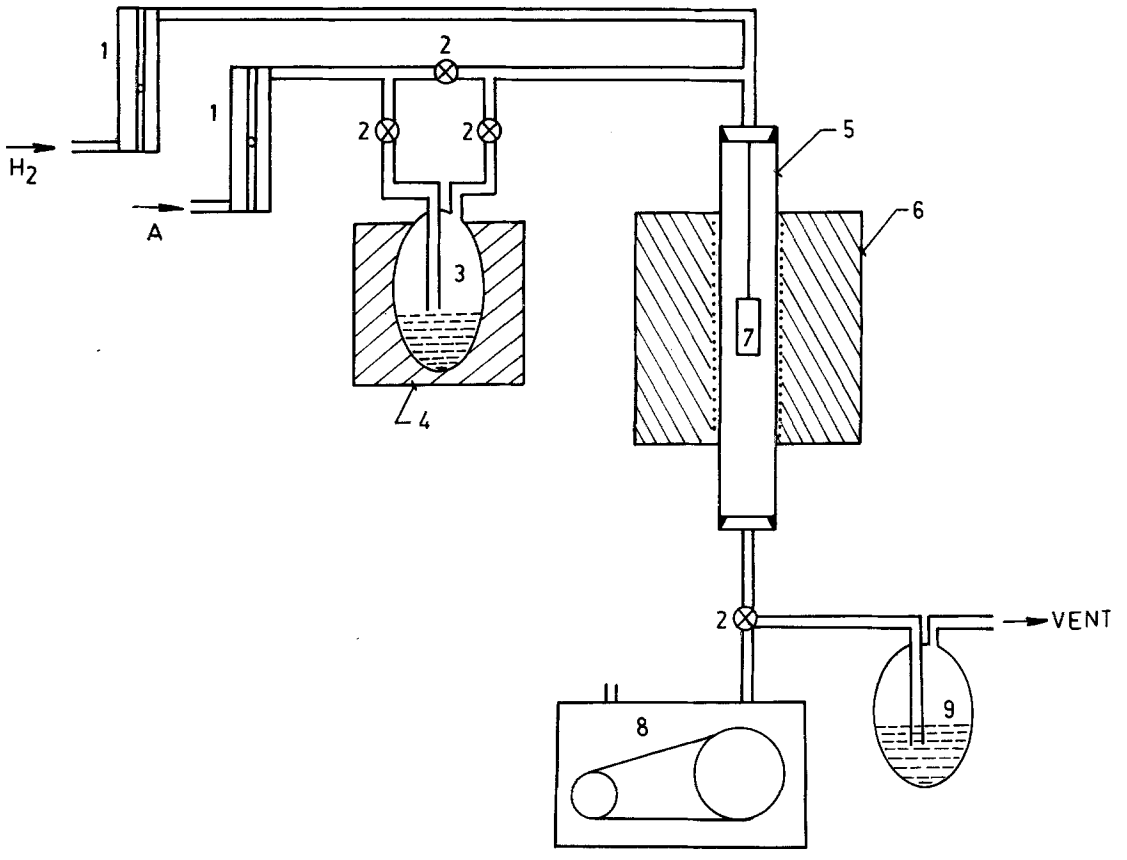

Figure 1 Schematic diagram of the experimental set-up. 1, flow meter; 2, PTFE stop-cock; 3, silicon tetrachloride bubbler; 4, low-temperature bath; 5, quartz reactor; 6, resistance furnace; 7, nickel substrate; 8, rotary pump; and 9, mineral oil bubbler.

using a Mettler thermogravimetric analysis (TGA) system with 0.01 mg sensitivity.

3. Results and discussion

3.1. Dependence of phase formation on the deposition parameters

In the present investigation, depending on the deposition conditions, two types of layers were formed on the surface: Type I consists of solid solution of silicon in nickel and Type II shows several phases. Table I presents the d-spacing against intensity values from a diffractogram obtained with a typical Type I coating. The peaks correspond to pure nickel with increased lattice parameter indicating a solid solution of silicon in nickel. Table II presents d-values obtained from a diffractogram representative of a silicon-enriched layer with several phases (Type II coating). The corresponding d-values for these several phases from the phase diagram of Ni–Si (see Fig. 2) [5] are also shown in Table II. It is clear from Table II that the phases β-Ni_3Si, γ-Ni_5Si_2, δ-Ni_2Si, ζ-Ni_3Si_2, η-NiSi and θ'-$NiSi_2$ are all present in the Type II coating. It is very well established that preferential orientation is usually found in CVD deposits. Hence, the intensity values can vary very widely for the deposits compared to well-annealed samples. Because of this, the relative intensity values are not presented for comparison in Table II.

TABLE I d-spacing values against intensity values, I/I_0, for typical Type I coating and for pure nickel

Type I coating		ASTM card values for pure nickel	
d	I/I_0	d	I/I_0
2.306	100	2.304	100
1.765	53	1.762	42
1.250	21	1.246	21

Table II shows the dependence of phase formation on the deposition parameters. It is reported earlier [1, 2] that only β-Ni_3Si and γ-Ni_5Si_2 form when pure nickel is siliconized. Wahl and Furst [2] report that coatings with higher silicon con-

TABLE II Comparison of d-values for Type II coating and for several nickel–silicon phases

d-spacing values from Type II coating	d-spacing values from ASTM cards					
	β-Ni_3Si	γ-Ni_5Si_3	δ-Ni_2Si	ξ-Ni_3Si_2	η-NiSi	θ'-$NiSi_2$
3.37		3.34		3.34		
3.258			3.26			
3.11						3.13
2.96						2.97
2.92		2.93		2.913		
2.84			2.86		2.84	
2.737			2.73			
2.637				2.634		
2.612		2.613				
2.48	2.49					2.48
2.278		2.26	2.28			
2.197		2.18	2.18			
2.16		2.15				
2.115			2.12			
2.068		2.05	2.06			
2.04		2.04	2.03	2.038	2.03	2.04
1.98		1.97	1.98	1.97	1.97	1.98
1.936				1.94		1.94
1.883		1.87			1.89	
1.85			1.85	1.84		
1.788			1.79			
1.769		1.77				
1.7592	1.751			1.755	1.75	1.75
1.678		1.669		1.672		
1.659		1.652	1.65			
1.639		1.631				1.64
1.607	1.609	1.609				
1.597		1.588			1.59	
1.55	1.569		1.56			
1.523		1.533	1.54		1.53	
1.50			1.51		1.51	1.51
1.47					1.46	
1.449	1.434					
1.409			1.40		1.39	1.39
1.386						1.38
1.376			1.37		1.37	
1.359			1.36			
1.347					1.35	1.35
1.323			1.324		1.32	
1.298					1.29	1.28
1.265			1.26			1.26
1.257					1.25	1.25
1.249						1.24
1.238	1.234					
1.232			1.23		1.23	1.23
1.22			1.22		1.21	1.21
1.205					1.20	
1.183			1.18			1.18
1.169	1.167		1.17		1.17	
1.16					1.16	
1.157			1.15		1.15	
1.124			1.12		1.12	
1.11			1.11		1.10	1.10
1.094			1.09		1.09	
1.08					1.08	
1.065			1.07		1.06	1.06

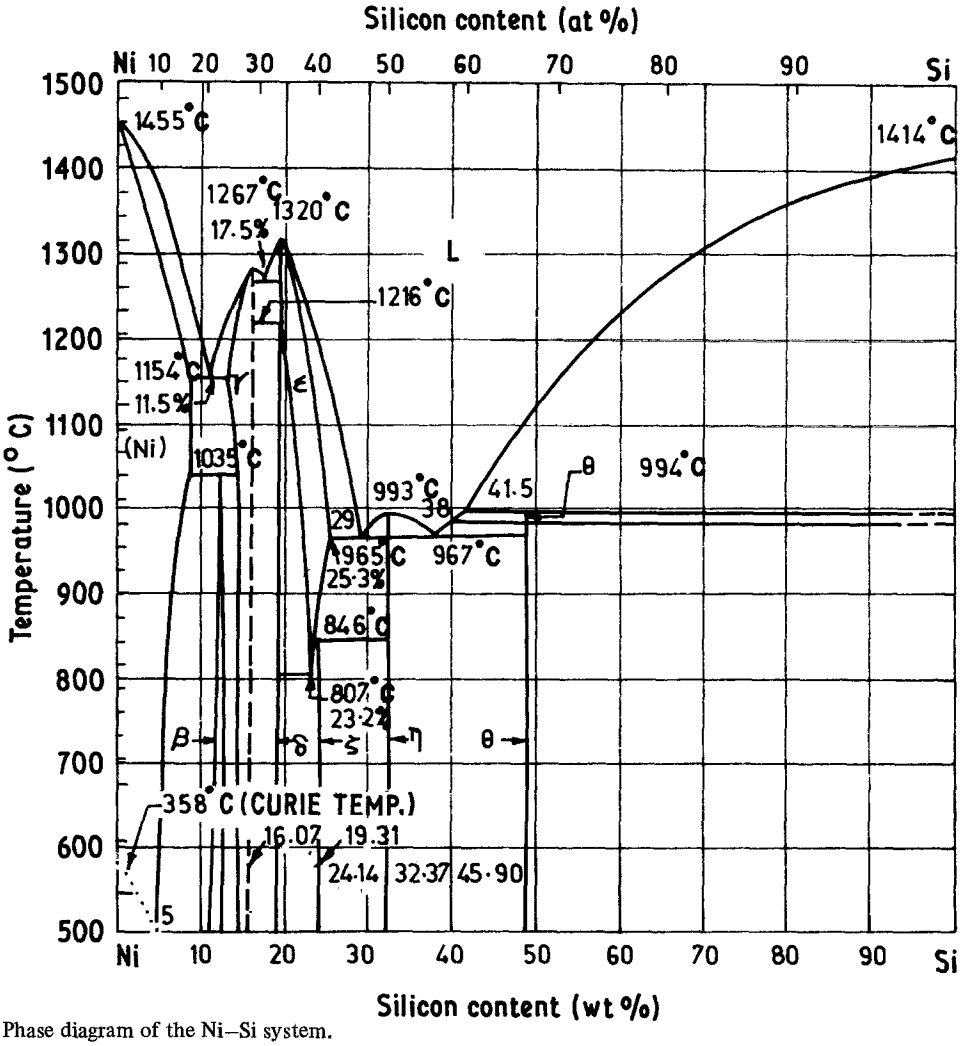

Figure 2 Phase diagram of the Ni–Si system.

tent form only during glow-discharge siliconizing. Table III shows the deposition conditions required to obtain phases with higher silicon content using a hot-wall reactor. Annealing these coatings for 8 h at 1000° C had not shown any change in X-ray diffraction.

From Table III it is evident that at low temperatures and low silicon tetrachloride partial pressures, solid solution of silicon in nickel forms. At high temperatures and high silicon tetrachloride partial pressures, the deposits formed contained several phases. At 1000° C and low partial pressures

TABLE III Dependence of phase formation on the deposition parameters

Sample number	Substrate temperature (°C)	Gas composition (partial pressure)			Deposition time (min)	Type of deposit
		p_{H_2}	p_{Ar}	$p_{Si\,Cl_4}$		
1	950	0.8653	0.1298	0.0049	30	Solid-solution
2	1000	0.9382	0.0595	0.0023	30	Solid-solution
3	1000	0.8168	0.1797	0.0034	30	Solid-solution
4	1000	0.8653	0.1298	0.0049	30	Solid-solution
5	1000	0.8168	0.1797	0.0034	60	Several phases
6	1000	0.8445	0.1498	0.0057	30	Several phases
7	1050	0.8168	0.1797	0.0034	30	Several phases
8	1050	0.8880	0.1123	0.0036	90	Several phases
9	1080	0.8880	0.1123	0.0036	120	Several phases

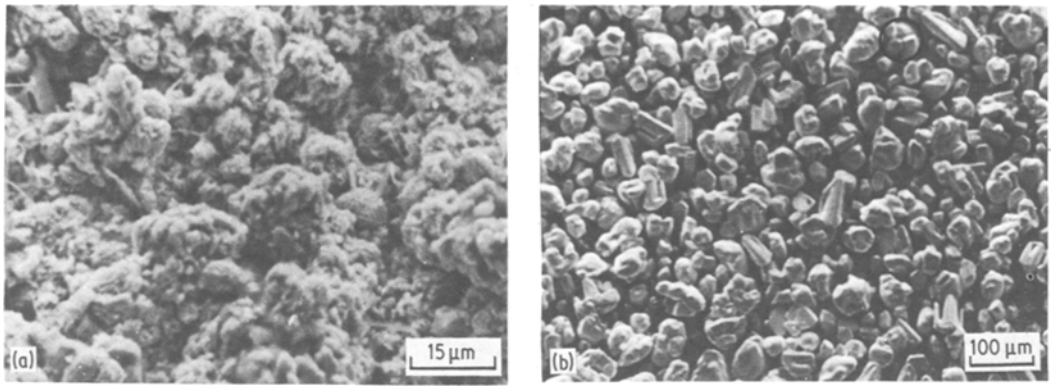

Figure 3 Surface morphology of silicon-coated nickel, Type II coating (several phases): (a) initial stages, (b) final stages.

of silicon tetrachloride, relatively longer times are required to form a layer with several phases.

3.2. Surface morphology and microstructure of deposits

Surface morphology of the solid-solution layers does not show any observable difference compared to the original substrate morphology. Fig. 3 shows the surface morphology of the Type II coating. In the early stages of the depositon process flower-like formations are evident (Fig. 3a). Finally, the layer builds into a stone-like morphology with a particle size of 50 to 60 μm (Fig. 3b).

The deposition of a silicon-enriched layer on the surface of a substrate can be conceived to form in the following steps:

(a) formation of silicon nuclei on the surface;

(b) diffusion of deposited silicon into the substrate;

(c) sequential precipitation of phases with higher silicon content as the thickness of the coating reaches a limit; and

(d) diffusion of nickel out into the coating.

The morphology follows these steps as the coating develops on the surface. Initially, a large number of nuclei form on the surface. Once the nuclei cover the entire area of the surface, inward diffusion of silicon takes place. As the silicon deposition continues on the surface, sequential precipitation of phases with higher silicon content occurs. At this stage the surface morphology of the silicon-enriched layer can be represented by Fig. 3a. The flower-like formations in Fig. 3a take further silicon and sinter together to form particles. The higher silicon-content phases, η-NiSi and θ'-$NiSi_2$, melt at 1000° C, as can be seen from the phase diagram (see Fig. 2). With the precipitation of these phases, a sintering process is favoured due to probable liquid-phase sintering. Smaller particles coalesce together to form larger particles of 50 to 60 μm in size, as shown in Fig. 3b. In the region shown in Fig. 3b, four particles sintering together and particles in various stages of sintering can clearly be seen.

A cross-section of the silicon-coated nickel substrate is shown in Fig. 4. Kirkindall porosity at the interface indicates the outward diffusion of nickel into the coating.

3.3. Oxidation characteristics

Fig. 5 shows results from short-time oxidation tests conducted on pure nickel and silicon coated nickel. The layer with solid solution of silicon in nickel shows improved oxidation resistance compared to the layer with several phases.

Fig. 6 shows the electron-probe microanalysis of nickel, silicon and oxygen across the interface of oxidized, silicon-coated substrate. This coating is of Type II. Three distinct zones can be seen: original substrate nickel, silicide layer and the oxide layer. The silicon composition was calcu-

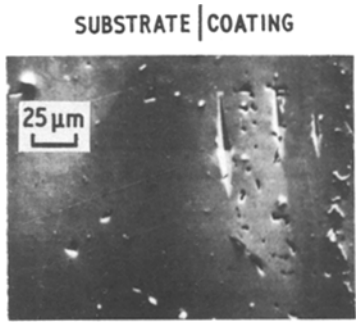

Figure 4 Cross-section of a silicon-coated nickel substrate.

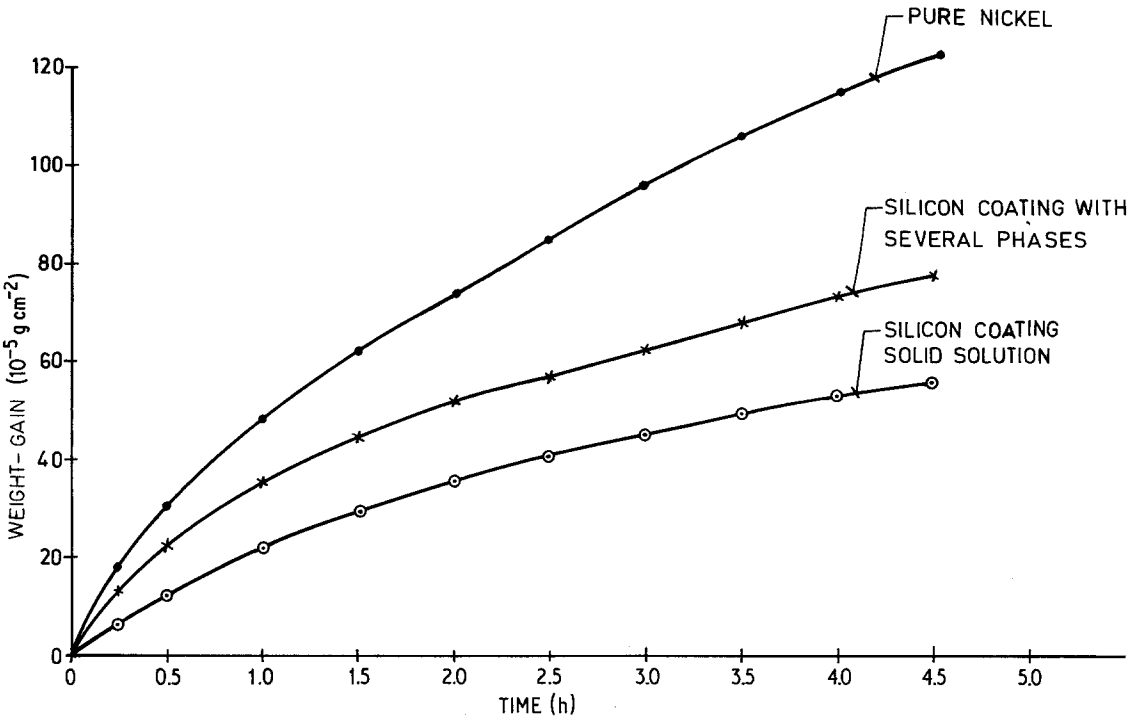

Figure 5 Weight-gain plotted against time curves for pure nickel and silicon-coated nickel.

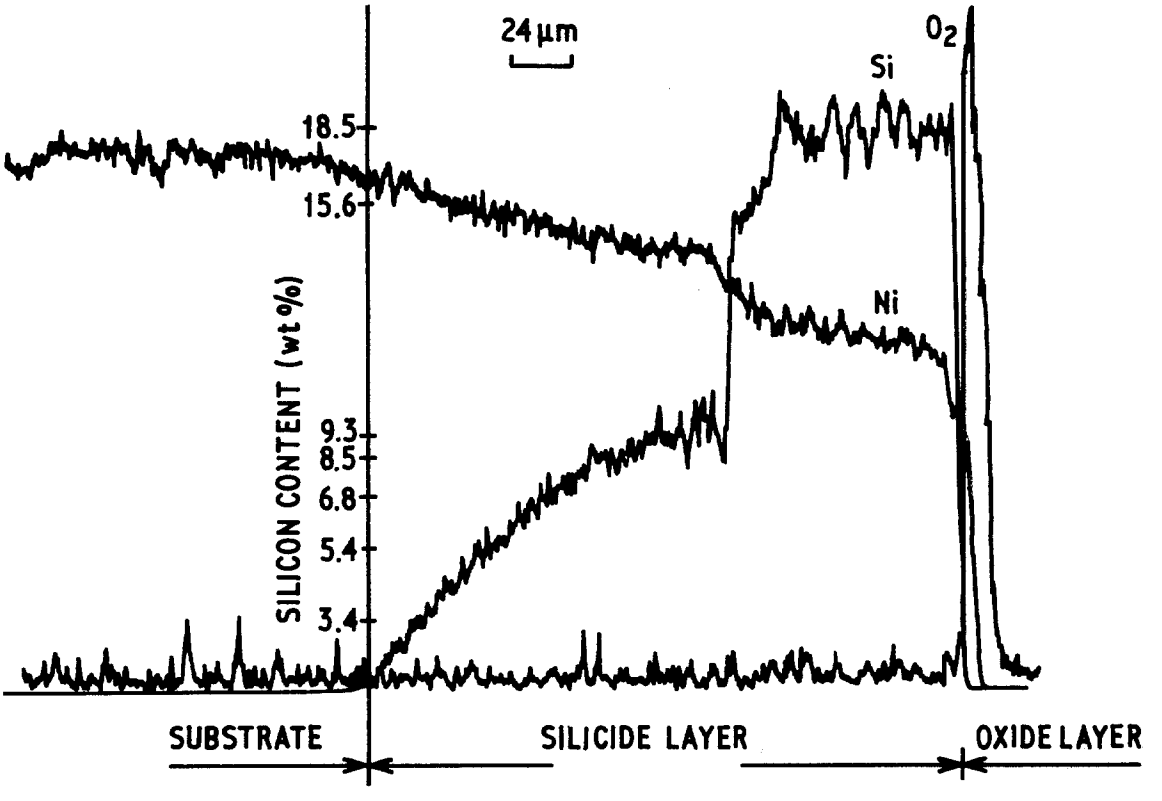

Figure 6 Electron-probe microanalysis across the interface of oxidized silicon-coated nickel.

lated from the measured intensities using a MAGIC computer program.

It can be seen in Fig. 6 that, in addition to the solid solution region, two phases exist in the coating, one with 15.6 wt% Si and another with 18.5 wt% Si. The oxide layer has the following composition: Ni, 62.7 wt%; Si, 3.9 wt%; and O, 29.0 wt%. This indicates that, on the surface, nickel is preferentially oxidized compared to silicon. In the early stages of oxidation of aluminum-coated nickel this type of preferential oxidation of nickel also occurs [6].

4. Conclusions

(a) Silicon-enriched layers are developed on pure nickel substrates by hydrogen reduction of silicon tetrachloride in the temperature range 950 to 1080° C. At low temperatures and low silicon tetrachloride partial pressures only solid solution of silicon in nickel forms on the surface. At higher temperatures (> 1000° C) and high silicon tetrachloride partial pressures, coatings formed contain all the phases present in the phase diagram.

(b) Surface morphologies of the layers with solid solution are smooth, without any observable change with deposition. Coatings with several phases show flower-like morphologies to begin with, ultimately leading to a stone-like morphology with a particle size of 50 to 60 μm. This could be due to liquid-phase sintering on the surface.

(c) Short-time oxidation tests indicate improvement in the oxidation resistance of silicide layers compared to nickel. The analysis of oxide layer shows that preferential oxidation of nickel occurs on the surface.

Acknowledgements

The author would like to thank Mr S. C. Mohan for the X-ray diffraction work and Mr J. A. Chowdary for the SEM work. He wishes to thank Mr P. Narasayya for his help in the experimental work. The author would like to thank the BHEL management for permitting publication of this work.

References

1. H. VAN AMERONGEN, in "High Temperature Alloys for Gas Turbines" edited by D. Contsouradis, P. Felix, H. Fischmeister, L. Habraken, Y. Lindblom and M. O. Speidel (Applied Science Publishers Ltd, London, 1978) pp. 209–224.
2. G. WAHL and B. FURST, in "Materials and Coatings to Resist High Temperature Corrosion" edited by D. R. Holmes and A. Rahmel (Applied Science Publishers Ltd, London, 1978) pp. 333–351.
3. P. C. FELIX and H. BENTLER, in Proceedings of the Third International Conference on Chemical Vapor Deposition, Salt Lake City, Utah, 1972, edited by F. A. Glaski (The American Nuclear Society, Hinsdale, Illinois, 1972) pp. 600–617.
4. A. R. NICOLL, U. W. HILDEBRANDT and G. WAHL, *Thin Solid Films* **64** (1979) 321.
5. "Metals Handbook: Metallography, Structures and Phase Diagrams" Vol. 8, 8th edn, edited by T. Lyman (American Society for Metals, Metals Park, Ohio, 1973) p. 325.
6. D. P. WHITTLE, in "High Temperature Alloys for Gas Turbines" edited by D. Coutsouradis, P. Felix, H. Fischmeister, L. Habraken, Y. Lindblom and M. O. Speidel (Applied Science Publishers Ltd, London, 1978) pp. 109–123.

Received 21 August
and accepted 30 November 1981